Aalborg Universitet

AALBORG UNIVERSITY

Fracture Energy of Plain Concrete Beams at Different Rates of Loading

Ulfkjær, J. P.; Hansen, Lars Pilegaard; Madsen, S. H.

Publication date:
1996

Document Version
Early version, also known as pre-print

Link to publication from Aalborg University

Citation for published version (APA):
Ulfkjær, J. P., Hansen, L. P., & Madsen, S. H. (1996). *Fracture Energy of Plain Concrete Beams at Different Rates of Loading*. Dept. of Building Technology and Structural Engineering, Aalborg University. Fracture and Dynamics Vol. R9610 No. 74

General rights
Copyright and moral rights for the publications made accessible in the public portal are retained by the authors and/or other copyright owners and it is a condition of accessing publications that users recognise and abide by the legal requirements associated with these rights.

- Users may download and print one copy of any publication from the public portal for the purpose of private study or research.
- You may not further distribute the material or use it for any profit-making activity or commercial gain
- You may freely distribute the URL identifying the publication in the public portal -

Take down policy
If you believe that this document breaches copyright please contact us at vbn@aub.aau.dk providing details, and we will remove access to the work immediately and investigate your claim.

Downloaded from vbn.aau.dk on: August 23, 2025

INSTITUTTET FOR BYGNINGSTEKNIK
DEPT. OF BUILDING TECHNOLOGY AND STRUCTURAL ENGINEERING
AALBORG UNIVERSITET • AUC • AALBORG • DANMARK

FRACTURE & DYNAMICS
PAPER NO. 74

To be presented at the Conference "Structures under Shock and Impact"
Voine, Italy, July 3-5, 1996

J. P. ULFKJÆR, L. PILEGAARD HANSEN, S. QVIST, S. H. MADSEN
FRACTURE ENERGY OF PLAIN CONCRETE BEAMS AT DIFFERENT RATES OF LOADING
MARCH 1996

ISSN 1395-7953 R9610

The FRACTURE AND DYNAMICS papers are issued for early dissemination of research results from the Structural Fracture and Dynamics Group at the Department of Building Technology and Structural Engineering, University of Aalborg. These papers are generally submitted to scientific meetings, conferences or journals and should therefore not be widely distributed. Whenever possible reference should be given to the final publications (proceedings, journals, etc.) and not to the Fracture and Dynamics papers.

Printed at Aalborg University

INSTITUTTET FOR BYGNINGSTEKNIK
DEPT. OF BUILDING TECHNOLOGY AND STRUCTURAL ENGINEERING
AALBORG UNIVERSITET • AUC • AALBORG • DANMARK

FRACTURE & DYNAMICS
PAPER NO. 74

To be presented at the Conference "Structures under Shock and Impact"
Voine, Italy, July 3-5, 1996

J. P. ULFKJÆR, L. PILEGAARD HANSEN, S. QVIST, S. H. MADSEN
FRACTURE ENERGY OF PLAIN CONCRETE BEAMS AT DIFFERENT RATES OF LOADING
MARCH 1996 ISSN 1395-7953 R9610

Fracture Energy of Plain Concrete Beams at Different Rates of Loading

J. P. Ulfkjær (*), L. P. Hansen (*), S. Qvist (**) and S. H. Madsen (**)

(*) Aalborg University, DK-9000 Aalborg, Denmark.

(**) DEMEX Consulting Engineers A/S, DK-2400 Copenhagen, Denmark.

Abstract

A simple experimental investigation is performed to measure how different fracture parameters of concrete are dependent on the displacement rate. One of the simplest structural geometries plain concrete beams with a notch in the midsection subjected to three point bending is used as test specimen. The beams are tested in a closed loop servo controlled materials testing system. The experimental results for these preliminary tests show that the bending tensile strength is increasing with the displacement rate and that the fracture energy is constant at lower displacement rates and then increasing at higher displacement rates. Further tests will be carried out.

1. Introduction

During the last two decades designers and inventors have been going to the limits of the codes by inventing new types of materials, H.H. Bache[2], and new types of structures subjected to a variety of loads such as wave loads and impact loads, Modéer, M.[2].

When using these types of structures, normal design philosophy can no longer be applied and it is therefore necessary to use more complicated and more realistic models.

For concrete structures, especially the fracture mechanical materials model, the Fictitious Crack Model by Hillerborg, Modéer and Petersson[4] has been acknowledged and is now used as a research tool and when designing huge

offshore structures, Modéer[6], and for concrete structures subjected to impact loads, Broadhouse[3].In these analyses the constitutive parameters are based on static tests and there is presently only little knowledge as to how these parameters are dependent on the strain rate.

Similar experiments have been performed by Mindess[7], but in those tests only the fracture toughness was determined.

In this paper a series of beams is tested at different displacement rates, and some fracture parameters are evaluated.

2. Materials and Test Set-up

2.1 Materials

A normal strength concrete/mortar is tested. The mix of the concrete is shown in table 1. The compressive strength, the Poisson ratio and the Young modulus in compression were determined on 100 mm by 200 mm cylinders. The tensile strength, the Young modulus and the Poisson ratio in tension were determined on a bone type of specimen with a smallest cross-section of 36 mm x 36 mm. In table 2 the mechanical properties of the concrete are shown.

Table 1. Mix of the concrete, units are kg/m^3.

Contents	Amount
Cement	437.1
Water	290.7
Sand (0-4 mm)	1484.3

Table 2. Mechanical parameters of the concrete.

Property	Number of test	Mean	Coefficient of Variation
Compressive strength	9	49.4 MPa	6.19 %
Youngs's modulus in compression	3	33600 MPa	1.45 %
Poissons ratio in compression	3	0.22	49.0 %
Tensile strength	2	2.89 MPa	0.90 %
Young modulus in tension	3	43500	16.9 %
Poisson's ratio in tension	1	0.145	-

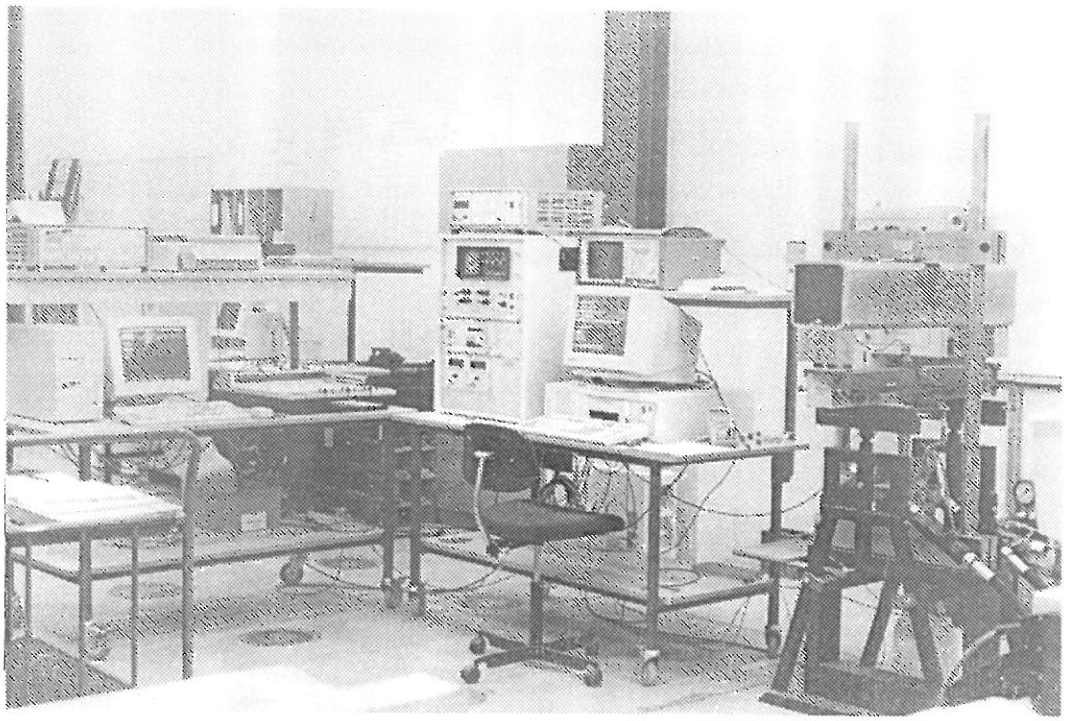

Figure 1. Photo of the test set-up.

2.2. Specimens

The standard RILEM specimen, RILEM-50FMC[8] for determination of fracture energy with the dimensions: span 800 mm, depth 100 mm and thickness 100 mm were used. The beams were cast in steel moulds. In total, twelve steel moulds were available at the same time. The day after casting the specimens were de-moulded and stored in water at 20°C until the day of testing. The day before testing a notch of half the beam depth was diamond saw cut in the beam. The beams were kept wet until the moment of testing. Six different displacement rates were used giving two experiments at every displacement rate.

2.3 Testing Equipment and Testing Procedure

The beams were subjected to three-point bending in a servo-controlled testing system. The beams were tested perpendicular to the casting direction. To measure the true beam deflection a reference bar was placed on either side of the beam and the deflection was measured using two LVDTs with a base of 2.0 mm and a sensitivity of 5.0 V/mm. The beam deflection was taken as the difference of the distance between the load point and the reference bar. The mean value of the two displacement transducers was used as the beam displacement. The piston displacement, the stroke, was measured using the built-in LVDT with a base of 5.0 mm and a sensitivity of 2.0 V/mm. The crack

only applicable to un-notched beams it should only be taken as a normalization of the peak load. The bending tensile strength for each beam is shown in Table 3. In figure 6 the bending tensile strength is plotted as a function of the logarithm of the displacement rate and it is seen that there is a linear relationship.

3.2 The Fracture Toughness

The fracture toughness (critical stress intensity factor) is determined according to linear elastic fracture mechanics using the relation, ASTM[1]:

$$K_c = \sigma_b \sqrt{a_i} f\left(\frac{a_i}{d}\right) \tag{3}$$

where:

$$f\left(\frac{a_i}{d}\right) = 1.93 - 3.07\left(\frac{a_i}{d}\right) + 14.53\left(\frac{a_i}{d}\right)^2 - 25.11\left(\frac{a_i}{d}\right)^3 + 25.8\left(\frac{a_i}{d}\right)^4 \tag{4}$$

The fracture toughness for each beam is shown in Table 3. Since the fracture toughness here is only a constant multiplied by the bending tensile strength the same tendencies are seen for the fracture toughness as for the bending tensile strength.

3.3 The Fracture Energy

The fracture energy is determined according to the fictitious crack model, Hillerborg, Modéer, and Petersson[4], and is here performed as in the RILEM recommendation, RILEM TC-50[8], except that the load is applied in the opposite direction to the gravity.

Different areas are calculated in connection with the RILEM method. The experiments are usually ended before the load is reduced to zero. The experiment will therefore end at the load, F_1, and the corresponding displacement, δ_1, and the remaining area under the load displacement curve must be estimated. In Ulfkjær and Brincker (1995) this area is shown to be:

$$A_1 = \frac{F_1 \delta_1}{t(d - a_i)} \tag{5}$$

The fracture energy is then determined as the area under the displacement curve divided by the ligament area plus A_1. The fracture energy for each beam is shown in Table 3. In figure 7 the fracture energy is plotted as a function of the logarithm of the displacement rate. It is seen that the fracture energy is independent of the fracture energy at lower displacement rates and increasing at the highest displacement rates.

opening displacement was measured over the initial notch using a clip gage with a base of 2.0 mm and with a sensitivity of 5.0 V/mm. The force was measured using a 10.0 kN load cell with a sensitivity of 1.0 kN/V. A photo of the test set-up is shown in figure 1.

The data acquisition system was a DMC9012A system from HBM connected to a personal computer. The force and the above-mentioned displacements were measured simultaneously so there is no time lag between the measurements. For the small loading rate (2.0E-3 mm/s, see table 4) the sampling rate was 2 Hz and for the high loading rate (3.4 mm/s, see table 4) the sampling rate was 9600 Hz.

The feed back signal, *FB*, was created by analogy addition of the corresponding signals:

$$FB = \delta_{Stroke} + 3\delta_{COD} \quad (1)$$

where δ_{Stroke} is the piston displacement and δ_{COD} is the crack opening displacement.

The reference signal, a linear ramp, was generated using a second AT PC and a digital to analogy converter. The rate of the reference signal determined the speed of the loading. A third AT-PC was used to control the position of the piston before the load was applied .

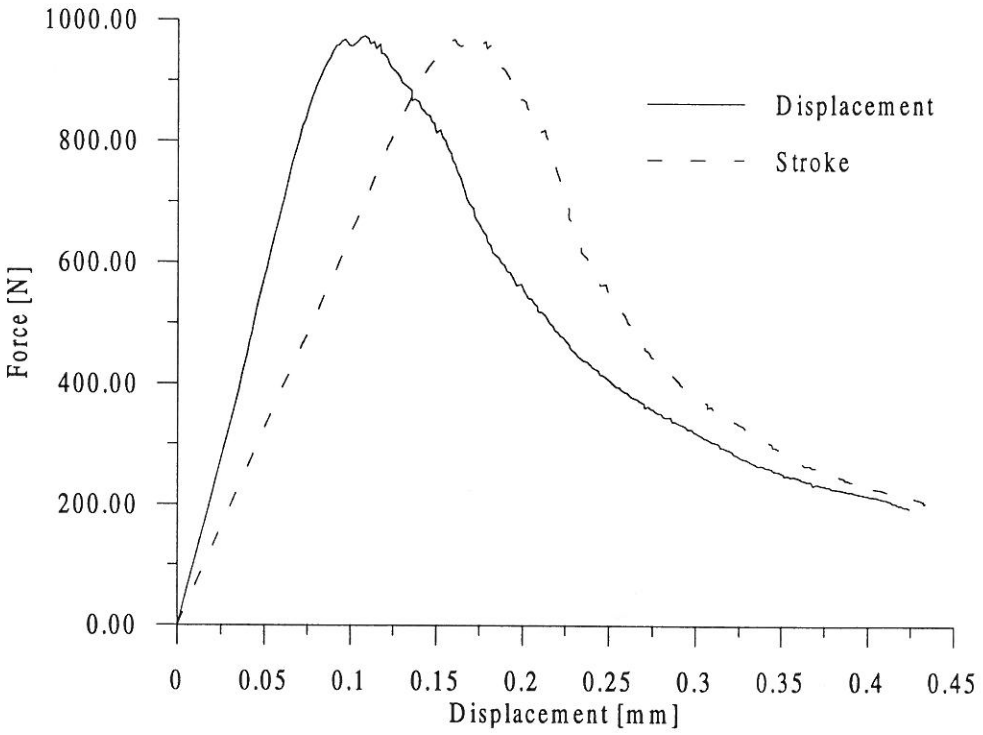

Figure 2. Difference between displacements measured using the reference bar and the built in LVDT for experiment No. 5 with a displacement rate of 3.6 E-2 mm/s.

3 Fracture Parameter Results

The first measurement of the force is from the dead load of the specimen. The subsequent measurements of the force include contributions from both the dead load and the applied load. In the calculations the distributed dead load has to be converted into a concentrated load. This is done by subtracting half the dead load from the measured load. In the following results this reduction has been done.

The importance of measuring the beam displacement using a reference bar is illustrated in figure 2, where the beam displacement and the stroke are plotted. It is seen that the displacement measured using the LVDT build in the cylinder is approximately 70% larger than the true beam displacement.

The first two tests were assumed to be quasi static. Then the speed of the reference signal was multiplied by a factor of four and two more tests were performed and so on giving six different displacement rates.

Load displacement curves for three different displacement rates are shown in figures 3-5. It is seen that the two repetitions are almost identical and that the peak load is increasing with the displacement rate.

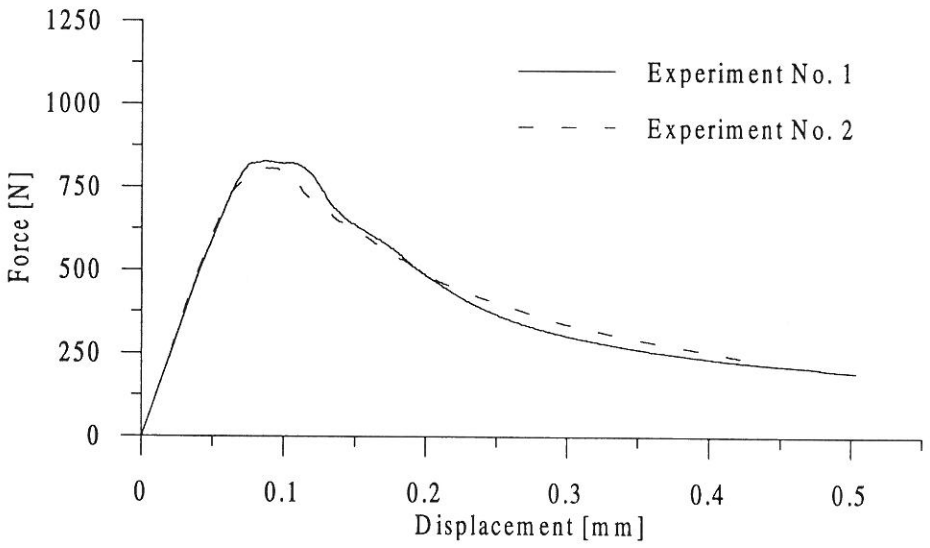

Figure 3. Load displacement curves for the first two experiments. The displacement rate is approximately 2.0 E-3 mm/s.

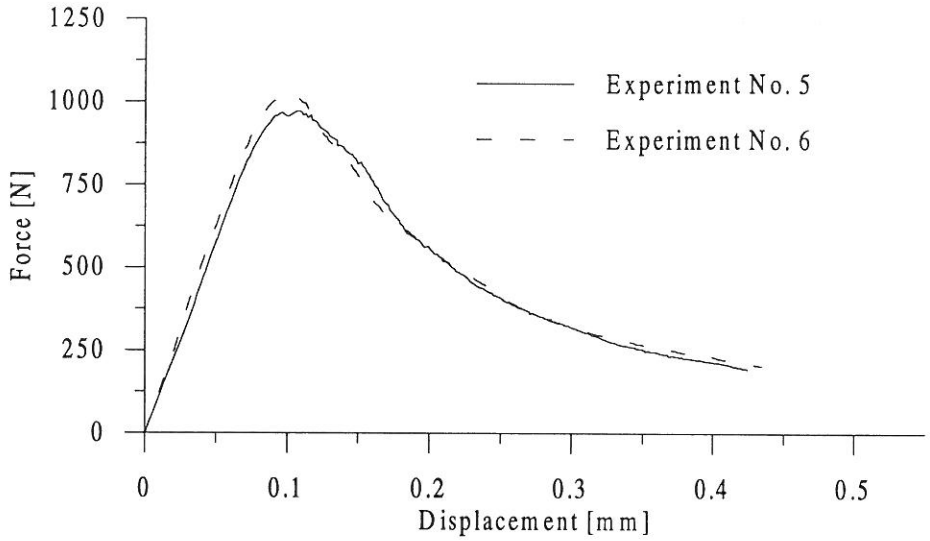

Figure 4. Load displacement curves for the fifth and sixth experiment. The displacement rate is approximately 3.6 E-2 mm/s.

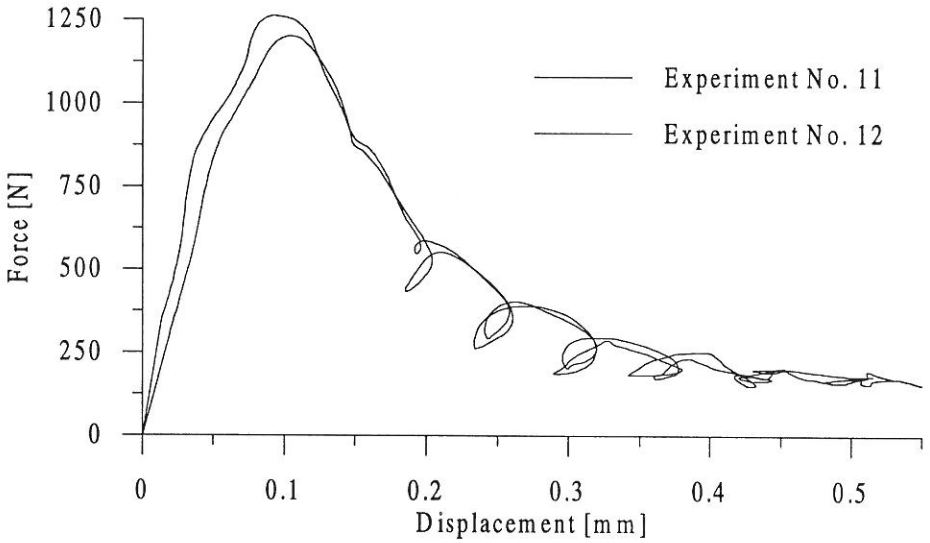

Figure 5. Load displacement curves for the last two experiments. The displacement rate is approximately 3.4 mm/s.

In figure 6 the time-displacement curve and the time-stroke curve are shown for experiment No. 5. It is seen that the speed of the beam displacement is almost constant which is not the case for the stroke.

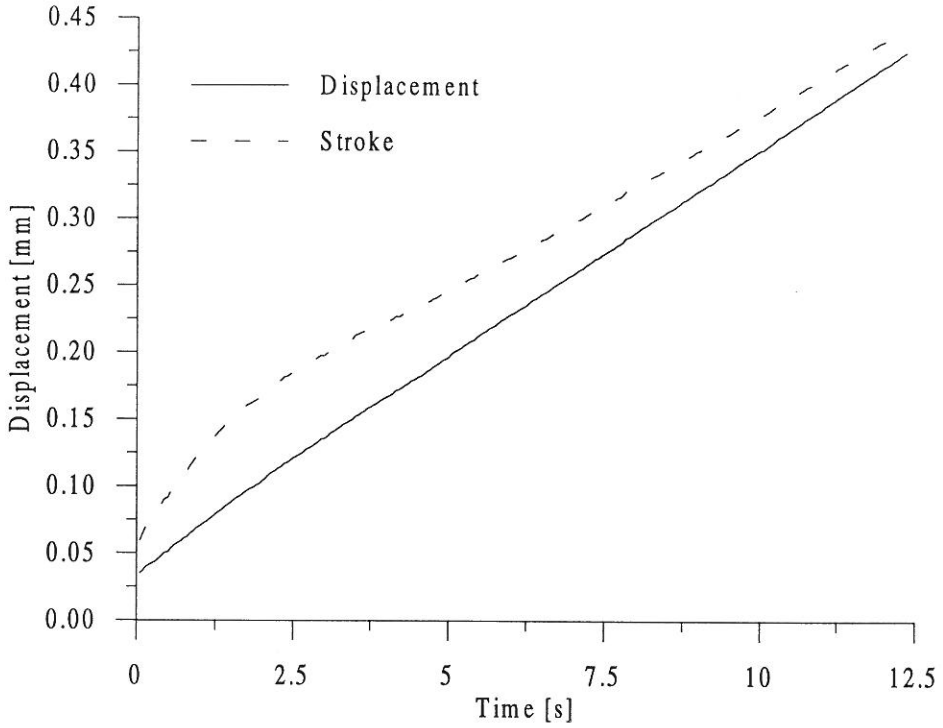

Figure 6. Difference of the displacement rate of the beam displacement and the stroke for experiment No. 5.

The displacement rate is calculated as the slope of the time-stroke curve where the slope is determined by calculating the best fit of the first 50 measurements using the least square method.

The following fracture parameters are calculated from the test results:

The Bending tensile strength according to Bernoulli.
The Fracture toughness according to Linear Elastic Fracture Mechanics
The Fracture Energy according to the Fictitious Crack Model

The fracture parameters for the six different displacement rates are shown in table 3.

3.1 The Bending Tensile Strength

The bending tensile strength was calculated according to Bernoulli theory, even though the beams have a notch in the midsection. The expression used is

$$\sigma_b = \frac{6P_{\max}L}{4(d-a_i)^2 t} \qquad (2)$$

where P_{max} is the peak load, L is the span of the beam, d is the beam depth, a_i is the depth of the initial notch and t is the beam thickness. As this equation is

only applicable to un-notched beams it should only be taken as a normalization of the peak load. The bending tensile strength for each beam is shown in Table 3. In figure 6 the bending tensile strength is plotted as a function of the logarithm of the displacement rate and it is seen that there is a linear relationship.

3.2 The Fracture Toughness

The fracture toughness (critical stress intensity factor) is determined according to linear elastic fracture mechanics using the relation, ASTM[1]:

$$K_c = \sigma_b \sqrt{a_i} f\left(\frac{a_i}{d}\right) \tag{3}$$

where:

$$f\left(\frac{a_i}{d}\right) = 1.93 - 3.07\left(\frac{a_i}{d}\right) + 14.53\left(\frac{a_i}{d}\right)^2 - 25.11\left(\frac{a_i}{d}\right)^3 + 25.8\left(\frac{a_i}{d}\right)^4 \tag{4}$$

The fracture toughness for each beam is shown in Table 3. Since the fracture toughness here is only a constant multiplied by the bending tensile strength the same tendencies are seen for the fracture toughness as for the bending tensile strength.

3.3 The Fracture Energy

The fracture energy is determined according to the fictitious crack model, Hillerborg, Modéer, and Petersson[4], and is here performed as in the RILEM recommendation, RILEM TC-50[8], except that the load is applied in the opposite direction to the gravity.

Different areas are calculated in connection with the RILEM method. The experiments are usually ended before the load is reduced to zero. The experiment will therefore end at the load, F_1, and the corresponding displacement, δ_1, and the remaining area under the load displacement curve must be estimated. In Ulfkjær and Brincker (1995) this area is shown to be:

$$A_1 = \frac{F_1 \delta_1}{t(d - a_i)} \tag{5}$$

The fracture energy is then determined as the area under the displacement curve divided by the ligament area plus A_1. The fracture energy for each beam is shown in Table 3. In figure 7 the fracture energy is plotted as a function of the logarithm of the displacement rate. It is seen that the fracture energy is independent of the fracture energy at lower displacement rates and increasing at the highest displacement rates.

Table 3. Fracture parameters at six different displacement rates.

	Displacement Rate		Bending Tensile Strength		Fracture Toughness		Fracture Energy	
	mm/s		MPa		$N/mm^{3/2}$		N/mm x 10^3	
1	2.0E-3	2.0E-3	4.09	3.94	17.98	17.41	61	59.5
2	2.0E-3		3.79		16.83		58	
3	8.3E-3	8.6E-3	4.27	4.36	18.94	19.25	56	53.5
4	8.9E-3		4.44		19.56		51	
5	3.7E-2	3.6E-2	4.84	4.80	21.27	21.72	59	59.5
6	3.6E-2		4.76		22.16		60	
7	1.4E-1	1.4E-1	5.11	5.08	22.72	22.53	48	59.5
8	1.4E-1		5.04		22.33		71	
9	6.7E-1	7.0E-1	5.61	5.60	24.97	24.82	79	73.5
10	7.3E-1		5.56		24.66		68	
11	3.6	3.4	6.16	5.90	27.13	26.10	81	84.5
12	3.2		5.63		25.07		88	

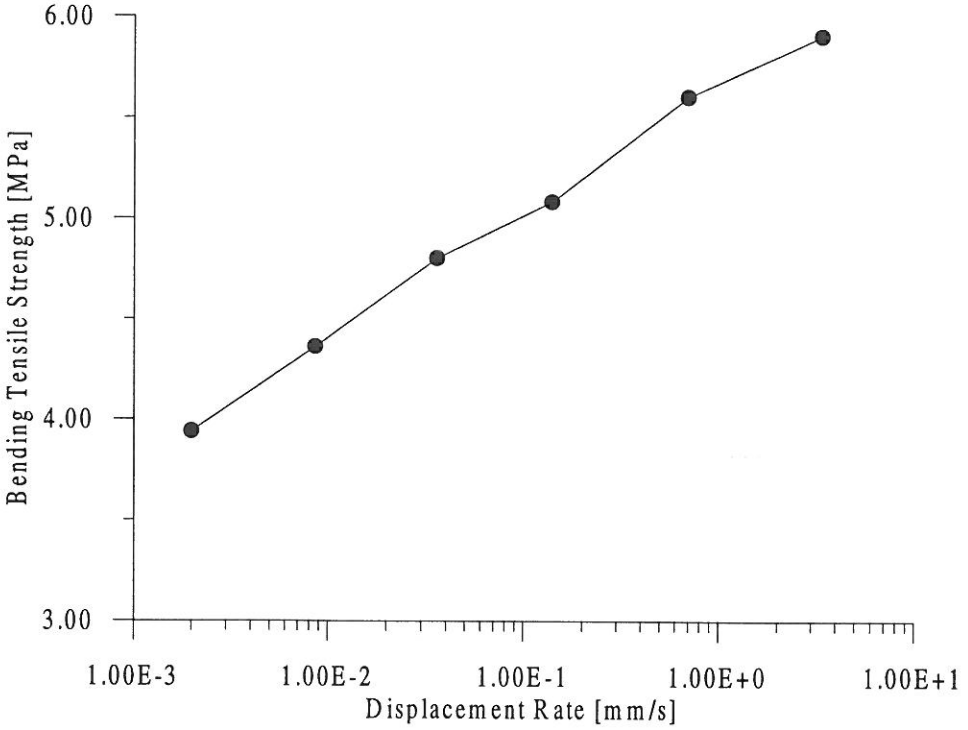

Figure 7. The bending tensile strength as a function of the displacement rate.

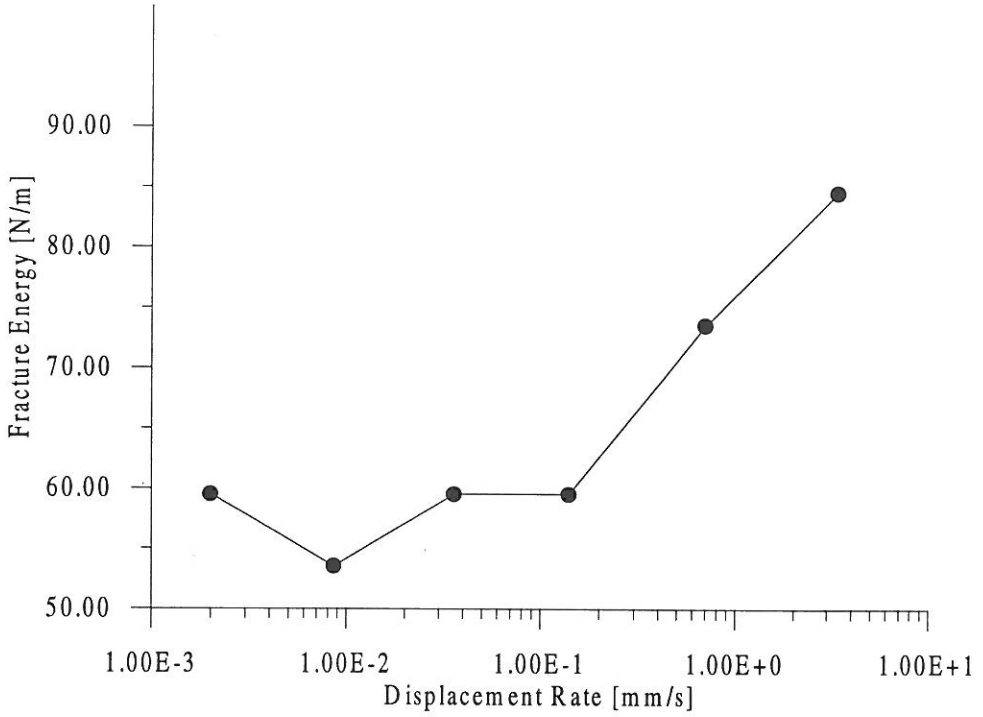

Figure 8 .The fracture energy as a function of the displacement rate.

4. Conclusions

A normal strength concrete/mortar was tested at six different displacement rates in order to determine how three fracture parameters of plain concrete beams in three point bending depend on the displacement rate. Three different fracture parameters were determined and the experimental results show that the bending tensile strength and the fracture toughness are increasing with the displacement rate and that the fracture energy is constant at lower displacement rates and then increasing for higher displacement rates. Further testing is necessary.

5. Acknowledgements

The financial support from the Danish Technical Research Council is greatly acknowledged.

6. References

1. ASTM E399-74: Method of test for plain strain fracture toughness of metallic materials, 1974.

2. Bache, H. H. Concrete and Concrete Technology in a Broad Perspective, in *Modern Design of Concrete Structures*, Invited lecture (Organisers Jens Peder Ulfkjær and Matz Modéer), Aalborg University, Aalborg, pp.1-47, ,

ISSN 0902-7513 R9513, 1995.

3. Broadhouse, B .J., DYNA3D Analysis of Cone Crack Formation due to Heavy Dropped Loads on Reinforced Concrete Floors, *in Structures Under Shock and Impact II* Editor P. S. Bulson, Computer Mechanics Publications, Thomas Telford, Portmouth, UK, pp. 285-296, 1992.

4. Hillerborg, A., Modéer, M. and Petersson, P. E., Analysis of crack formation and Crack Growth in Concrete by Means of Fracture Mechanics and Finite Elements, *Cement and Concrete Research*, 6, 773-782, 1976.

5. Modéer, M., Offshore Concrete Platforms in Norway - Materials and Static Analysis, in *´Fracture of Brittle Disordered Materials: Concrete, Rock and Ceramics'* (Editors, G. Baker and B. L. Karihaloo), Queensland, Australia. 1993.

6. Modéer, M., Modern Design in Practice, *in Modern Design of Concrete Structures* (Organisers Jens Peder Ulfkjær and Matz Modéer), Aalborg University, Aalborg, 145-154, ISSN 0902-7513 R9513, 1995.

7. Mindess, S., Rate of Loading Effects on the Fracture of Cementitious Materials, in *Application of Fracture Mechanics to Cementitious Composites* (Edited by S. P. Shah), Evanston, Illinois, pp. 617-636, (1985).

8. RILEM 50-FMC, Determination of the Fracture Energy of Mortar and Concrete by Means of Three Point Bend Test on Notched Beams, *Materials and Structures*, Vol. 18, No. 106, pp. 285-290. (1985)

9. Ulfkjær, J. P. and Brincker R. Fracture Energy of Normal Strength Concrete, High Strength Energy and Ultra High Strength Ultra Ductile Steel Fibre Reinforced Concrete, *in Fracture Mechanics of Concrete Structures* (Editor: Wittmann), Aedificatio Publishers, Vol. 1., pp. 31-44, 1995.

FRACTURE AND DYNAMICS PAPERS

PAPER NO. 61: R. Brincker, P. Andersen, P. H. Kirkegaard, J. P. Ulfkjær: *Damage Detection in Laboratory Concrete Beams.* ISSN 0902-7513 R9458.

PAPER NO. 62: R. Brincker, J. Simonsen, W. Hansen: *Some Aspects of Formation of Cracks in FRC with Main Reinforcement.* ISSN 0902-7513 R9506.

PAPER NO. 63: R. Brincker, J. P. Ulfkjær, P. Adamsen, L. Langvad, R. Toft: *Analytical Model for Hook Anchor Pull-out.* ISSN 0902-7513 R9511.

PAPER NO. 64: P. S. Skjærbæk, S. R. K. Nielsen, A. Ş. Çakmak: *Assessment of Damage in Seismically Excited RC-Structures from a Single Measured Response.* ISSN 1395-7953 R9528.

PAPER NO. 65: J. C. Asmussen, S. R. Ibrahim, R. Brincker: *Random Decrement and Regression Analysis of Traffic Responses of Bridges.* ISSN 1395-7953 R9529.

PAPER NO. 66: R. Brincker, P. Andersen, M. E. Martinez, F. Tallavó: *Modal Analysis of an Offshore Platform using Two Different ARMA Approaches.* ISSN 1395-7953 R9531.

PAPER NO. 67: J. C. Asmussen, R. Brincker: *Estimation of Frequency Response Functions by Random Decrement.* ISSN 1395-7953 R9532.

PAPER NO. 68: P. H. Kirkegaard, P. Andersen, R. Brincker: *Identification of an Equivalent Linear Model for a Non-Linear Time-Variant RC-Structure.* ISSN 1395-7953 R9533.

PAPER NO. 69: P. H. Kirkegaard, P. Andersen, R. Brincker: *Identification of the Skirt Piled Gullfaks C Gravity Platform using ARMAV Models.* ISSN 1395-7953 R9534.

PAPER NO. 70: P. H. Kirkegaard, P. Andersen, R. Brincker: *Identification of Civil Engineering Structures using Multivariate ARMAV and RARMAV Models.* ISSN 1395-7953 R9535.

PAPER NO. 71: P. Andersen, R. Brincker, P. H. Kirkegaard: *Theory of Covariance Equivalent ARMAV Models of Civil Engineering Structures.* ISSN 1395-7953 R9536.

PAPER NO. 72: S. R. Ibrahim, R. Brincker, J. C. Asmussen: *Modal Parameter Identification from Responses of General Unknown Random Inputs.*ISSN 1395-7953 R9544.

PAPER NO. 73: S. R. K. Nielsen, P. H. Kirkegaard: *Active Vibration Control of a Monopile Offshore Structure. Part One - Pilot Project.* ISSN 1395-7953 R9609.

PAPER NO. 74: J. P. Ulfkjær, L. Pilegaard Hansen, S. Qvist, S. H. Madsen: *Fracture Energy of Plain Concrete Beams at Different Rates of Loading.* ISSN 1395-7953 R9610.

Department of Building Technology and Structural Engineering
Aalborg University, Sohngaardsholmsvej 57, DK 9000 Aalborg
Telephone: +45 98 15 85 22 Telefax: +45 98 14 82 43

FRACTURE AND DYNAMICS PAPERS

PAPER NO. 44: A. Rytter: *Vibrational Based Inspection of Civil Engineering Structures.* Ph.D.-Thesis. ISSN 0902-7513 R9314.

PAPER NO. 45: P. H. Kirkegaard & A. Rytter: *An Experimental Study of the Modal Parameters of a Damaged Steel Mast.* ISSN 0902-7513 R9320.

PAPER NO. 46: P. H. Kirkegaard & A. Rytter: *An Experimental Study of a Steel Lattice Mast under Natural Excitation.* ISSN 0902-7513 R9326.

PAPER NO. 47: P. H. Kirkegaard & A. Rytter: *Use of Neural Networks for Damage Assessment in a Steel Mast.* ISSN 0902-7513 R9340.

PAPER NO. 48: R. Brincker, M. Demosthenous & G. C. Manos: *Estimation of the Coefficient of Restitution of Rocking Systems by the Random Decrement Technique.* ISSN 0902-7513 R9341.

PAPER NO. 49: L. Gansted: *Fatigue of Steel: Constant-Amplitude Load on CCT-Specimens.* ISSN 0902-7513 R9344.

PAPER NO. 50: P. H. Kirkegaard & A. Rytter: *Vibration Based Damage Assessment of a Cantilever using a Neural Network.* ISSN 0902-7513 R9345.

PAPER NO. 51: J. P. Ulfkjær, O. Hededal, I. B. Kroon & R. Brincker: *Simple Application of Fictitious Crack Model in Reinforced Concrete Beams.* ISSN 0902-7513 R9349.

PAPER NO. 52: J. P. Ulfkjær, O. Hededal, I. B. Kroon & R. Brincker: *Simple Application of Fictitious Crack Model in Reinforced Concrete Beams. Analysis and Experiments.* ISSN 0902-7513 R9350.

PAPER NO. 53: P. H. Kirkegaard & A. Rytter: *Vibration Based Damage Assessment of Civil Engineering Structures using Neural Networks.* ISSN 0902-7513 R9408.

PAPER NO. 54: L. Gansted, R. Brincker & L. Pilegaard Hansen: *The Fracture Mechanical Markov Chain Fatigue Model Compared with Empirical Data.* ISSN 0902-7513 R9431.

PAPER NO. 55: P. H. Kirkegaard, S. R. K. Nielsen & H. I. Hansen: *Identification of Non-Linear Structures using Recurrent Neural Networks.* ISSN 0902-7513 R9432.

PAPER NO. 56: R. Brincker, P. H. Kirkegaard, P. Andersen & M. E. Martinez: *Damage Detection in an Offshore Structure.* ISSN 0902-7513 R9434.

PAPER NO. 57: P. H. Kirkegaard, S. R. K. Nielsen & H. I. Hansen: *Structural Identification by Extended Kalman Filtering and a Recurrent Neural Network.* ISSN 0902-7513 R9433.

PAPER NO. 58: P. Andersen, R. Brincker, P. H. Kirkegaard: *On the Uncertainty of Identification of Civil Engineering Structures using ARMA Models.* ISSN 0902-7513 R9437.

PAPER NO. 59: P. H. Kirkegaard & A. Rytter: *A Comparative Study of Three Vibration Based Damage Assessment Techniques.* ISSN 0902-7513 R9435.

PAPER NO. 60: P. H. Kirkegaard, J. C. Asmussen, P. Andersen & R. Brincker: *An Experimental Study of an Offshore Platform.* ISSN 0902-7513 R9441.